Neural Comput & Applic (2019) 31:1127–1142
DOI 10.1007/s00521-017-3143-0

ORIGINAL ARTICLE

Modified multiple generalized regression neural network models using fuzzy C-means with principal component analysis for noise prediction of offshore platform

Cheng Siong Chin[1] · Xi Ji[1] · Wai Lok Woo[1] · Tiaw Joo Kwee[2] · Wenxian Yang[1]

Received: 15 February 2016 / Accepted: 27 June 2017 / Published online: 12 July 2017

Abstract A modified multiple generalized regression neural network (GRNN) is proposed to predict the noise level of various compartments onboard of the offshore platform. With limited samples available during the initial design stage, GRNN can cause errors when it maps the available inputs to sound pressure level for the entire offshore platform. To obtain more relevant group for GRNNs training, fuzzy C-mean (FCM) is used. However, outliers in some group may interfere the prediction accuracy. The problem of selecting suitable inputs parameters (in each cluster) is often impeded by lack of accurate information. Principal component analysis (PCA) is used to ensure high relevance input variables in each cluster. By fusing multiple GRNNs by an optimal spread parameter, the proposed modeling scheme becomes quite effective for modeling multiple frequency-dependent data set (ranging from 125 to 8000 Hz) with different input parameters. The performance of FCM-PCA-GRNNs has improved significantly as the results show a 25% improvement on the spatial sound pressure level (SPL) and 85% improvement on the spatial average SPL than just GRNNs alone. By comparing with data obtained from real engine room on a jack-up rig, the FCM-PCA-GRNNs noise model performs better with around 16% less error than the empirical-based acoustic models. Additionally, the results show comparable performance to statistical energy analysis that requires more time and resources to solve during the early stage of the offshore platform design.

Keywords Fuzzy C-mean · Principal component analysis · Generalized regression neural network · Noise prediction · Offshore platform

1 Introduction

Noise control is an important aspect which ensures the crew habitability onboard offshore platform. Implementing noise prediction is an effective way to identify the potential noise problem at the early stage of offshore platform design to avoid expensive retrofitting cost in the later stage of modification. Currently, excessive noise in the offshore and marine applications is identified mainly using the empirical formula or the computer-aided design (CAD)-based mathematical tools. For example, the finite element analysis (FEA) and the boundary element method (BEM) solve acoustic responses by considering wave propagation; the statistical energy analysis (SEA) and the energy finite element analysis (EFEA) determine the sound field based on power flow between subsystems. However, the accuracy of the results could not be guaranteed [1] if the empirical formulas are applied to different applications as some formulas are unable to meet the necessary assumptions such as room's shape, room's size and sound source. On the other hand, the CAD-based numerical tool is proven to be quite accurate for certain frequency regime; however, using these tools for large scale system such as the offshore platform can be quite time and resource consuming.

For the past few decades, neural networks have been used to model complex systems. In machine learning, there are many methods available in the literature. In this study,

✉ Cheng Siong Chin
cheng.chin@ncl.ac.uk

[1] Faculty of Science, Agriculture and Engineering, Newcastle University, Newcastle NE1 7RU, UK

[2] Ngee Ann Polytechnic, Marine and Offshore Technology Centre of Innovation (MOT COI), 535 Clementi Rd, Singapore 599489, Singapore

a general regression neural network (GRNN) [2] is used. It is quite advantageous due to its ability to converge to the underlying function of the data after few training samples, and the results are quite consistent. A full knowledge of the system to be modeled is often not required. It makes GRNN a useful tool to perform prediction and comparison of system performance in practice. As a result, the noise engineers can spend more time on the noise analysis instead of creating an accurate CAD model that requires exact values of the model variables in the computer-based acoustic simulation.

Many applications including the noise-related applications [3–6] use GRNN. In the current literature, GRNN application on the offshore platform such as a jack-up rig has not been discussed. In addition, the inherent use of steels for room construction in the jack-up rig differs from most of the land-based industrial and acoustic rooms [7, 8] that increase the percentage of structure-borne noise than airborne noise. Moreover, the problems of selecting the appropriate inputs from the design variables (e.g., actual position of the noise sources, room dimensions, and other acoustic variables) are often impeded by a lack of exact information during the early design stage of the offshore platform. The relevant inputs used for GRNN training are often quite subjective, and the types of input variables used for training can vary across different noise engineers due to their experience.

Hence, a modified multiple GRNN using fuzzy C-means (FCM) clustering and principal component analysis (PCA) is proposed to predict the noise level on the jack-up rig with the least number of significant inputs. The training and test samples from 125 to 8000 Hz obtained from the computer-based statistical energy analysis (SEA) with direct field (SEA-DF) software approach validated by experimental data [9] will be used. These input data will be preprocessed by FCM and PCA to group the dominant samples together and reduce the dimensionality of the input variables before commencing the training using GRNN. With optimal spread variables obtained for each cluster at different frequencies, multiple GRNN can be fused to form an optimal GRNN. The proposed method enables noise engineers to predict the noise level on any similar offshore platform without repeating the SEA modeling that is often time and resource consuming.

The contributions of the paper are as follows. First, by fusing multiple GRNNs at different frequencies, the proposed modeling scheme is sufficient for modeling various frequency-dependent data that contain several input variables (as compared to current acoustic room models in the literature that do not consider the frequency variation, room geometry, source power, and receiver position in a single formula). With more relevant variables used in each cluster after the FCM-PCA, it consumes less computational time as compared to conventional GRNNs that applied to original data set with higher dimensions. Second, with multiple GRNNs training and FCM-PCA, it enhances the input variables selection and thus delivers more reliability and robustness to the overall noise prediction model.

This paper has the following sections. Section 2 describes the proposed noise prediction using FCM-PCA-GRNNs. Section 3 illustrates the selection of input variables for FCM-PCA-GRNNS. Sections 4 and 5 introduce the real offshore structure case study and the data preprocessing using FCM and PCA, respectively. Section 6 describes the design of multiple FCM-PCA-GRNNs. Section 7 shows the results and discussion. Section 8 concludes the paper.

2 Proposed noise prediction using FCM-PCA-GRNNs

The proposed approach uses a validated SEA-DF model [9] to train the FCM-PCA-GRNNs model. The neural networks determine the relationship between the room input parameters to the total spatial equivalent sound pressure level (SPL) and spatial average SPL at different [10] frequencies (e.g., 125–8000 Hz). The total equivalent SPL consists of both direct and diffuse field (or reverberant field) where the former is obtained via MATLAB™, and later by a commercial SEA modeling software called VA-One™. It is capable to compute both the airborne and structure-borne noise from the mid- to high-frequency range [10]. The total equivalent noise level is the logarithmic sum of both the direct field ($L_{p,\mathrm{dir}}$) and reverberant ($L_{p,\mathrm{rev}}$) component as shown.

$$L_{p,\mathrm{tot}} = 10\log\left(10^{0.1L_{p,\mathrm{dir}}} + 10^{0.1L_{p,\mathrm{rev}}}\right) \quad (1)$$

The proposed noise prediction architecture is shown in Fig. 1. The first layer (see the top of Fig. 1) models the reverberant field noise level and direct field noise level using VA-One™ and MATLAB™, respectively. The experimental validations of the total or equivalent noise levels are performed before the training of the neural network. The next layer (see the bottom of Fig. 1) requires the total equivalent SPL and the input parameters from the acoustic and structure features of the offshore platform compartments. The fuzzy C-means clustering on the available input data can help to identify clusters from the data set of 424 samples (for each frequency range 125, 250, 500, 1000, 2000, 4000, and 8000 Hz) to obtain a concise representation of a system's input–output behavior. The GRNN training is then performed on these clusters. If the spread parameter σ_0 can produce the desired results for the

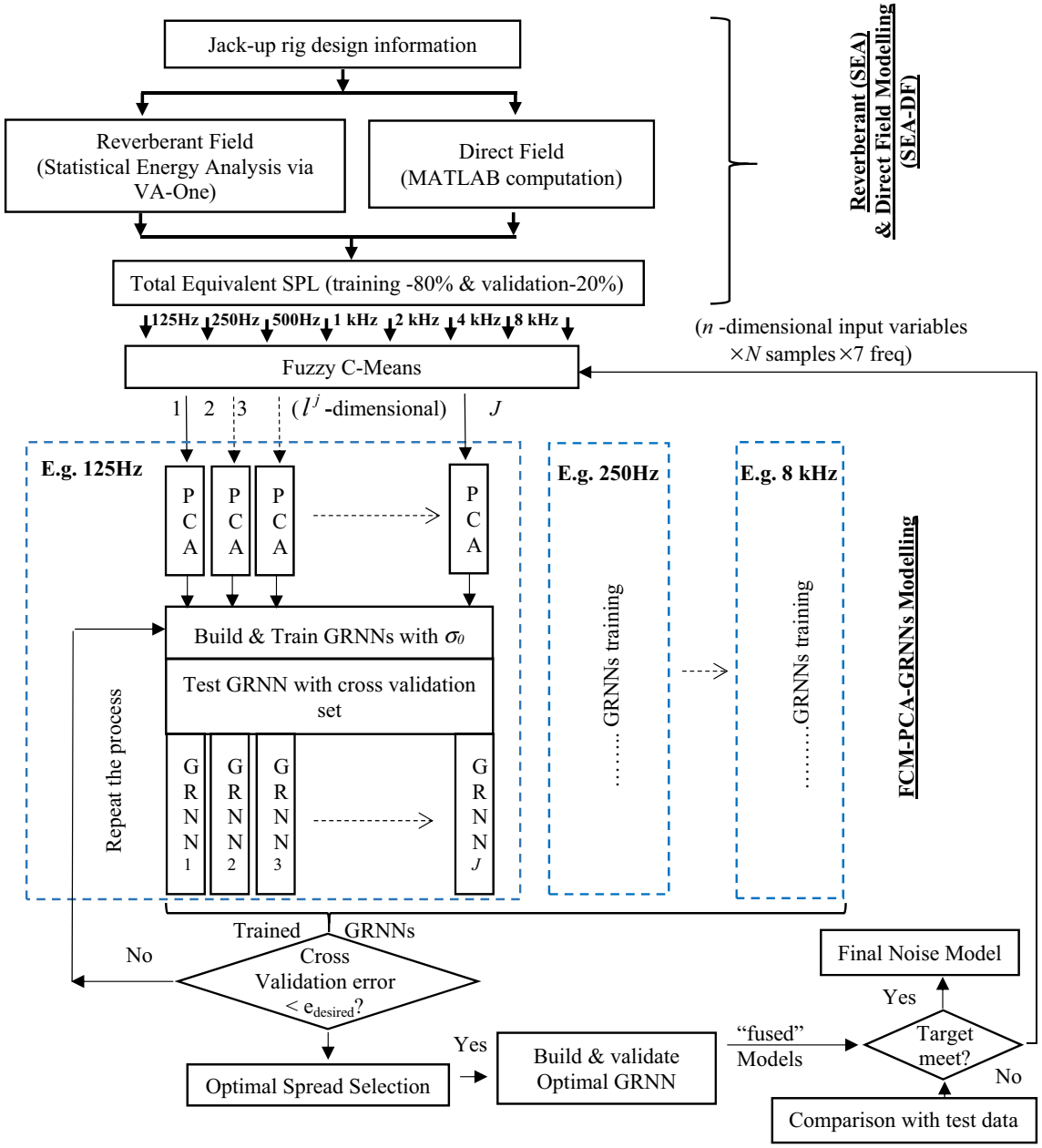

Fig. 1 Proposed architecture for noise prediction using FCM-PCA-GRNNs

cross-validation set, an updated spread parameter $\sigma_i = \sigma_0 + i \times \theta$ (where θ is the learning factor and i is the number of iteration) will be used. The optimization of spread parameter will terminate when the root mean squared error (RMSE) of the cross-validation set is less than the desired error. The final GRNNs will be built using the optimal spread parameter, followed by testing the results with a validation set and experimental data (if available). With the FCM-PCA-GRNNs model for each frequency established, it can predict the corresponding total equivalent SPL in any compartments on any similar type of offshore platform.

3 Selection of input parameters for FCM-PCA-GRNNs

The input variable for FCM-PCA-GRNNs training is selected based on two main principles: (1) parameters that describe the acoustics and structure features of the offshore platform, and (2) parameters that influence the response of the sound fields. This information will require a prior understanding of the acoustic problem on the board of the jack-up rig at a different frequency. In addition, the acoustic environment on the jack-up rig is quite complex due to its large number of noise and vibration sources

distributed quite closely within a compact space, and the use of wide variety of different materials for wall's construction. Noise is transmitted via an airborne and structure-borne transmission. The airborne noise governs the compartment's sound field where the high noise level machinery is concentrated. In general, the SPL measured in the airborne-dominated compartments can be approximated by the Heerema and Hodgson empirical formula [9, 11]. The formula used to determine the room sound pressure level is directly related to the room geometry, source power level, source–receiver distance, absorption coefficient, and fitting density of the source room.

The strong airborne noise in the source room can penetrate through the common bulkheads or decks to influence the noise in the adjacent rooms. The transmitted acoustic energy depends on the incident acoustic energy and transmission loss which is determined by the plate material properties and thickness as shown.

$$L_{\text{adj}} = L_{\text{source}} - R + 10\log\frac{S}{S\alpha} \tag{2}$$

where L_{adj} and L_{source} are the SPL of the adjacent room and source room, respectively. R and S are the transmission loss and surface area of the common bulkhead/deck, respectively. Here α is the mean absorption coefficient of the adjacent room. In some cases where the SPL within the source and the adjacent room is not known, the range of SPL is provided by the regulation, namely NORSOK S-002 for eight different room types based on the permitted noise levels onboard of the offshore platform as seen in Table 1.

On the other hand, the structure-borne sound is directly caused by vibrating machinery-induced mechanical force, or indirectly by the structure excitation due to incident airborne noise. The energy radiated by structures is proportional to the plate's radiation efficiency, surface area, density, sound propagation speed, and the square of plate vibration velocity. The structure-borne sound affected the remote rooms and attenuated as distance increases. The structure-borne SPL can be expressed as.

$$L_{SB} = L_V + 10\log\sigma + 10\log\frac{S\alpha}{4S} \tag{3}$$

where L_V denotes the structure vibration level, σ is the radiation efficiency, and S and α are the structure surface area and room absorption coefficient, respectively.

The acoustic field in the compartments behaves differently. For example, the machinery compartments contain airborne source radiation (e.g., engine room, mud pump room); structure-borne and transmission noise (e.g., workshops, stores); and airborne, structure-borne and transmission noise (e.g., pump room, transformer room). Due to the good isolation strategies and damping treatment, the SPL in the living quarter is usually dominated by the air-conditioning diffuser radiated noise. The mechanical diffusers are typically found in heating, ventilating, and air-conditioning systems (HVAC). Some room adjacent to the machinery compartments is affected by the transmitted structure-borne noise. As a result, the compartments in the offshore platform can be classified into five general groups:

- Compartments dominated by the airborne noise
- Compartments influenced by the structure-borne and transmission noise
- Compartments influenced by airborne and structure-borne noise
- Compartments influenced by airborne and transmission noise
- Compartments influenced by airborne, structure-borne and transmission noise simultaneously

Table 1 Room types defined for compartment onboard

Room Type (1 to 8)	Descriptions	Compartments	Permitted noise level (dBA)
1	Unmanned machinery room	Engine room, fire pump room, emergency generator room, and thruster room	110
2	Unmanned machinery room	AHU room	90
3	Manned machinery room	Switchboard room, transformer room, drill floor, mud room, mixing area, pipe rack, general process and utility area, pump room, and cement room	85
4	Unmanned instrument room	Local instrument room, electrical MCC room	75
5	Store, workshop, and instrument room	Mechanical/electrical workshop, paint store, LQ stores, dish washing	70
6	Living quarter public area	change room, LQ corridor, and toilets	60–65
7	Living quarter public area, laboratory, and local control room	Local control room, laboratory, galley, mess room, workshop office, gymnasium, and lobby	50–60
8	Cabin, hospital, and central control room	Cabin, hospital, and wheelhouse control room	45

Based on the above sound analysis, several main parameters that determine the spatial and spatial average SPL of the room on the offshore platform can be obtained. These includes the following 13 inputs and two output parameters: (1) total interior source power level; (2) room type; (3) room surface area; (4) room volume; (5) first nearest source sound power level; (6) source/receiver distance from the first source; (7) second nearest source sound power level; (8) source/receiver distance from the second source; (9) room mean absorption coefficient; (10) maximum sound power level of adjacent rooms; (11) panel or insulation thickness; (12) room type of the adjacent room; (13) number of decks to the main deck; (14) spatial SPL; and (15) average spatial SPL.

4 Case study on real offshore structure

The hull dimensions of the jack-up rig [9] involved in the study are approximately 88.8 m (length) × 115.1 m (width) × 12 m (height) as seen in Fig. 2a. There are four aspects of developing a SEA model: (a) the structure properties and configurations; (b) designed noise control treatment; (c) the source information; and lastly (d) the frequency range.

The offshore structures are mainly made of steels modeled by a ribbed plate with the specific properties in the construction drawing. The interior of each compartment in the offshore platform is treated as a "cavity" which represents one acoustic subsystem of SEA model. These air cavities together with structural subsystem such as six walls around the room are connected to one another by point, line, and surface area junctions which enable the energy flow within the entire SEA model. The sound pressure level, sound power level, and vibration level of equipment are obtained from the vendor during the factory acceptance test (FAT) at 100% of the nominal load. The absorbing effects of the applied insulation layers in all compartments are obtained from reverberation time (T60) measurement. For the damped acoustic spaces, the SEA model is based on the assumption of reverberant energy. It is important to separate the direct field component from the total energy. At steady-state condition, the final sound power injects to the reverberant field of the subsystem is as follows.

$$P_{\text{rev}}^{k} = (1 - \bar{\alpha}_k) P_{\text{in}}^{k} \tag{4}$$

where the reverberant sound power in subspace k denoted by P_{in}^{k} is reduced by a factor of $(1 - \bar{\alpha}_k)$. Here $\bar{\alpha}_k$ is the mean absorption of the subspace k.

The frequency range is set from 125 to 8000 Hz after examining the number of modes present in each subsystem within the compartment. After solving the SEA

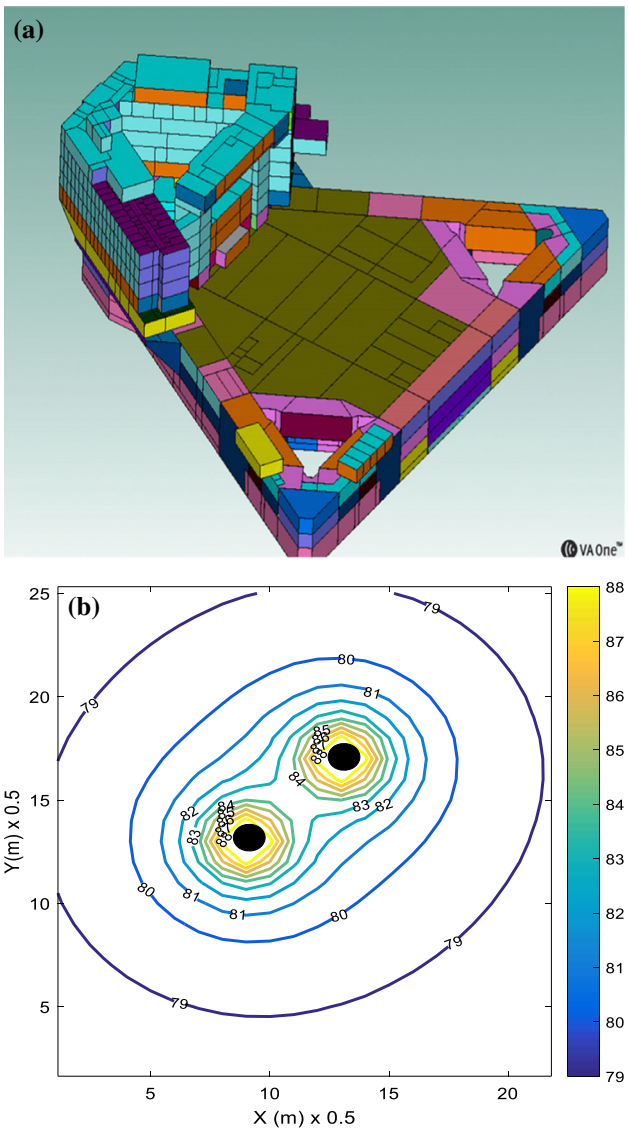

Fig. 2 **a** Statistical energy analysis model of jack-up rig (*color indicates level* of SPL), **b** SPL (in dB) of direct field from two pumps (indicated by *two black dots*) (color figure online)

energy balance equation of the jack-up rig, the reverberant SPL in each compartment is obtained. Due to the space limitation in the offshore platform compartments, equipment is distributed quite closely. The direct sound radiation from the equipment can also affect the equivalent SPL. Thus, the correct noise model of the equipment is crucial for the equivalent SPL. According to the literature [12], the marine equipment can be modeled by three types of the noise source. A point source has inverse square ($1/r^2$) attenuation for small- and medium-sized equipments such as compressors, pumps, and purifiers; a rectangular surface source will generate box-like shaped contours like large machinery such as main diesel generator, mud pumps, and hydraulic pumping unit (HPU). In this study, both the reverberant (see Fig. 2a) and direct

sound transmissions (see Fig. 2b) in the room are considered. The direct sound contribution from the adjacent rooms is neglected. The direct field component will be computed before adding to the reverberant field to obtain the total equivalent SPL using (1). A total number of 424 input and output samples at the seven frequencies are obtained from different rooms on the jack-up rig as shown in Fig. 2a. For clarity, the input and output range of these samples are tabulated in Table 2. Note that the above-mentioned thirteen input variables (see row 1–13) and two outputs (see last two rows) are used.

5 Data preprocessing using FCM-PCA

As discussed in Sect. 4, the sound transmission path in various compartments is different. By preprocessing the collected samples via data clustering can help to group samples into clusters of similar characteristics. The FCM algorithm [13, 14, 15] creates groups according to the distance between the data points and the cluster centers. Let x_i be input parameters at each frequency, e.g., 125, 250,…,8000 Hz. The input variables of n-dimensional are denoted by $\mathrm{X}_i = (x_1, x_2, \ldots, x_n) \in \Re^n, \forall i = 1, 2, \ldots, N$

Table 2 Input and output range for each input parameter

No.	Input variables and outputs	125 Hz		250 Hz		500 Hz		1000 Hz		2000 Hz		4000 Hz		8000 Hz	
		Max.	Min.	Max.	Min.	Max.	Min.	Max.	Min.	Max.	Min.	Max.	Min.	Max.	Min.
	Inputs														
1	Total interior sound power level (dBA)	104.6	0.0	115.2	0.0	122.0	0.0	128.0	0.0	123.0	0.0	122.0	0.0	114.0	0.0
2	Room type	8.0	1.0	8.0	1.0	8.0	1.0	8.0	1.0	8.0	1.0	8.0	1.0	8.0	1.0
3	Room surface area (m^2)	2052.0	39.2	2052.0	39.2	2052.0	39.2	2052.0	39.2	2052.0	39.2	2052.0	39.2	2052.0	39.2
4	Room volume, V (m^3)	2160.0	16.2	2160.0	16.2	2160.0	16.2	2160.0	16.2	2160.0	16.2	2160.0	16.2	2160.0	16.2
5	First nearest source sound power levels (dBA)	101.0	0.0	112.0	0.0	119.0	0.0	125.0	0.0	120.0	0.0	119.0	0.0	111.0	0.0
6	Source/receiver distance from the first source (m)	20.0	0.0	20.0	0.0	20.0	0.0	20.0	0.0	20.0	0.0	20.0	0.0	20.0	0.0
7	Second nearest source sound power levels (dBA)	101.0	0.0	112.0	0.0	119.0	0.0	125.0	0.0	120.0	0.0	119.0	0.0	111.0	0.0
8	Source/receiver distance from the second source (m)	20.2	0.0	20.2	0.0	20.2	0.0	20.2	0.0	20.2	0.0	20.2	0.0	20.2	0.0
9	Room mean absorption coefficient	0.3	0.0	0.6	0.0	0.7	0.0	0.6	0.0	0.6	0.0	0.5	0.0	0.5	0.0
10	Max sound power level of adjacent room (dBA)	104.6	0.0	115.2	0.0	122.0	0.0	128.0	0.0	123.0	0.0	122.0	0.0	114.0	0.0
11	Room type of adjacent room	8.0	1.0	8.0	1.0	8.0	1.0	8.0	1.0	8.0	1.0	75.0	1.0	8.0	1.0
12	Panel/insulation thickness between adjacent room (mm)	75.0	0.0	75.0	0.0	75.0	0.0	75.0	0.0	75.0	0.0	75.0	0.0	75.0	0.0
13	Number of decks to main deck	6.0	−2.0	6.0	−2.0	6.0	−2.0	6.0	−2.0	6.0	−2.0	6.0	−2.0	6.0	−2.0
	Outputs														
14	Spatial l SPL (dBA)	90.5	20.4	97.2	21.0	103.3	16.2	109.4	12.9	104.5	9.9	103.9	0.0	95.9	0.0
15	Spatial averaging SPL (dBA)	89.8	20.4	96.5	21.0	101.6	16.2	108.0	12.9	103.0	9.9	102.6	0.0	94.6	0.0

form the corresponding columns in the data matrix $\mathrm{X} = [\mathrm{X}_1, \mathrm{X}_2, \ldots, \mathrm{X}_N]^T \in \Re^{N \times n}$ where N is the number of samples for each frequency as shown in Fig. 3.

The FCM algorithm partitions the data matrix $\mathbf{X}$ into jth cluster (denotes as $\mathbf{X}^j$) for each frequency. A fuzzy partition represented as a matrix $\mathbf{U}$, with elements of u_{ji} - [0, 1], gives the membership degree in the partition. The fuzzy partitioning is carried out through an iterative optimization of the objective function in (7), with the update of membership for each frequency as

$$\mu_{ji} = \frac{\left(1/d^2(\mathrm{X}_i, v_j)\right)^{1/(m-1)}}{\sum_{j=1}^{J}\left(1/d^2(\mathrm{X}_i, v_j)\right)^{1/(m-1)}} \tag{5}$$

and cluster centers

$$v_j = \frac{\sum_{i=1}^{N}(\mu_{ji})^m \mathrm{X}_i}{\sum_{i=1}^{N}(\mu_{ji})^m}, \quad \forall j = 1, 2, \ldots, J \tag{6}$$

where v_j represents the center of jth cluster, m is the fuzziness index, and $m \in (1, \infty)$ determines the fuzziness of the clusters. The number of the cluster center is denoted by J. The Euclidean distance between ith data and jth cluster's center is $d(\mathrm{X}_i, v_j) = \left\|\mathrm{X}_i - v_j\right\|$, and μ_{ji} accounts for the membership of ith data to the center of jth cluster.

The main objective of the FCM algorithm is to minimize the objective function $J(\mathbf{X}; \mathbf{U}, \mathbf{V})$ on $\mathbf{U}$ and $\mathbf{V}$.

$$J(\mathbf{X}; \mathbf{U}, \mathbf{V}) = \sum_{j=1}^{J}\sum_{i=1}^{N}\mu_{ji}^m d(\mathrm{X}_i, v_j)^2, \quad 2 \le J < N \tag{7}$$

where $\mathbf{V} = (v_1, v_2, \ldots, v_J)$ is the cluster prototype to be determined and $\mathbf{U}$ is the fuzzy partition that must satisfy the following constraints:

$$\sum_{j=1}^{J}\mu_{ji} = 1, \forall i \text{ and } 0 < \sum_{i=1}^{N}\mu_{ji} = N, \forall j \tag{8}$$

The fuzzy cluster is obtained through an iterative optimization of (7) according to the unsupervised optimal fuzzy clustering.

After setting the number of clusters $J = 5$ and the maximum number of iterations as 200, the FCM algorithm is applied to all frequency samples. The clustering results are presented in Fig. 4a–g in the form of parallel coordinates plot to visualize and analyze multivariate data having different range and SI unit. The values of the thirteen input variables are polylines with vertices on the vertical axes. The numbers in the X-axis represent the thirteen input variables as seen in Table 2. The position of the vertex on the ith axis corresponds to the ith coordinate of the sample [16]. For example, there exists a higher value in the sixth and eighth input within cluster 5. These high values can be contributed by the possible noise [17] within samples

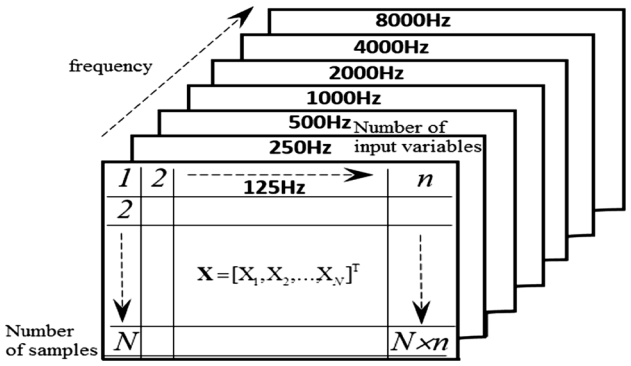

Fig. 3 Input data matrix in three-dimensional

collected. The sound samples which are close to the cluster centers are considered as normal samples. However, they are assigned with very low or zero membership in the cluster group. As a result, the PCA is used to reduce the dimensionality through finding the high relevance input variables for each cluster at a particular frequency.

The correlations of input variables to the outputs are quite different in each cluster. The input variable selection is implemented on the data matrix $\mathbf{X}$ in jth cluster (denotes as $\mathbf{X}^j$) for each frequency to reduce the input dimension. Note that the superscript "j" will be used to define jth cluster and subscript "i" refers to the index for each sample. PCA uses the singular value decomposition (SVD) to rank the input variables in descending order of importance to least important. The most important variables are given a higher priority than the less significant ones.

Briefly, the first step in the PCA algorithm is to normalize the components such that they have unity variance and zero means. It is followed by an orthogonalization method to determine the normalized principal components. The PCA operates on each cluster at particular frequency as follows.

1. Subtract the mean of each data point in the data set $\mathbf{X}^j$ to produce a data set of zero means in the cluster $j = 1, 2, \ldots, J$ denotes as

$$\mathbf{X}^j - \bar{\mathbf{X}}^j \tag{9}$$

where the mean $\bar{\mathbf{X}}^j = \sum_{i=1}^{N^j}\mathrm{X}_i^j/N^j$, X_i^j is the input samples, N^j is the number of samples in the jth cluster, respectively.

2. Compute the square covariance matrix $\mathbf{\Omega}^j$ of size $l \times l$ for jth cluster where l is the number of reduced input variables.
3. Perform singular value decomposition (SVD) on the covariance matrix $\mathbf{\Omega}^j$.

$$\mathbf{\Omega}^j = \bar{\mathbf{U}}^j \mathbf{S}^j \bar{\mathbf{V}}^{j\mathbf{T}} \tag{10}$$

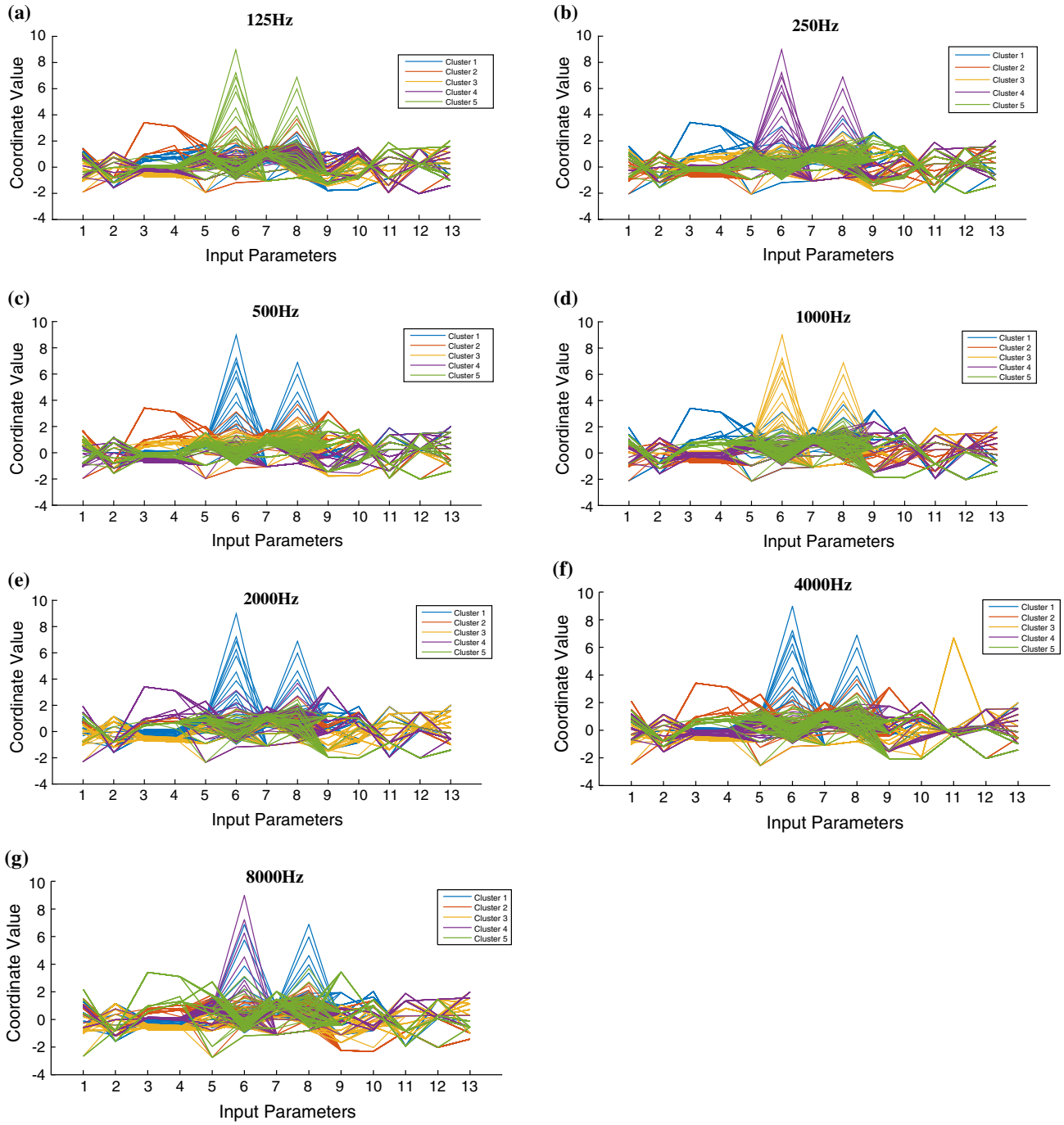

Fig. 4 **a** Data distribution at 125 Hz after FCM, **b** data distribution at 250 Hz after FCM, **c** data distribution at 500 Hz after FCM, **d** data distribution at 1000 Hz after FCM, **e** data distribution at 2000 Hz after FCM, **f** data distribution at 4000 Hz after FCM, and **g** data distribution at 8000 Hz after FCM

where $\bar{\mathbf{U}}^j$ is a $l \times l$ matrix with columns being orthonormal eigenvectors or left singular vectors of $\mathbf{\Omega}^j\mathbf{\Omega}^{j\mathrm{T}}$, $\bar{\mathbf{V}}^{j\mathrm{T}}$ is a $l \times l$ matrix with columns being orthonormal eigenvectors or right singular vectors of $\mathbf{\Omega}^{j\mathrm{T}}\mathbf{\Omega}^j$ and $\mathbf{S}^j = \mathrm{diag}(s_1, \ldots, \mathrm{s}_l)$ is a $l \times l$ diagonal matrix with the nonzero elements. It is also the singular values or the square roots of eigenvalues from $\bar{\mathbf{U}}^j$ or $\bar{\mathbf{V}}^j$ positioned in descending order.

4. Apply $\mathbf{U}^j$, $\mathbf{S}^j$, and $\mathbf{V}^j$ to determine the inverse square root of the covariance matrix.

$$\mathbf{\Omega}^{j-1/2} = \sum_{i=1}^{h} \frac{1}{\sqrt{\mathbf{S}_i^j}} \mathbf{U}_i^j \mathbf{V}_i^{j\mathrm{T}} \tag{11}$$

where h is the number of eigenvectors for eigenvalues in $\mathbf{S}^j$.

5. Multiply the SVD-computed inverse square root covariance matrix as shown to obtain the reduced dimensional data set.

$$\mathbf{\Omega}^{j-1/2}(\mathbf{X}^j - \bar{\mathbf{X}}^j) \tag{12}$$

Based on the acoustic field behavior in Sect. 4, the samples are grouped into five clusters at different center frequencies using the FCM. The PCA is then applied to each cluster to determine the number of principal components. In this study, the cumulative percentage of variance criteria is applied to determine the number of principal components. According to this criterion, principal components are chosen based on their cumulative proportion of variance higher than a prescribed threshold value of 95%. The leverage scores for each dimension are obtained by calculating their two norms. Figure 5 shows the norm for the thirteen input parameters at each frequency. The different heights shown on the respective bar charts reflect the dominant input parameters used for each cluster. The dominant input parameters are only retained in each cluster thus reduces the problem dimension and eliminates the relativity between the input parameters.

As shown in Fig. 5, the significant principal components are identified. The principal components below the predetermined threshold value are removed. The remaining input variables should contain the most dominant variables for GRNN training. Table 3 summarizes the result of Fig. 5, and "x" refers to variable removed while "o" refers to the dominant variables to retain for GRNN training. For example, the seven remaining input variables for cluster 1 at 125 Hz are the total sound power level, room surface area, room volume, nearest source#1 sound power level, nearest source#2 sound power level, maximum sound power level of adjacent room, and panel/insulation thickness between adjacent room. Due to the unsupervised characteristics of the FCM and application of PCA, the importance of the input variables (or a number of dominant parameters) in each cluster varies across the frequencies. Note that the reduced sample size used for the GRNN's training is different in each cluster for the frequencies.

6 Model of multiple GRNN after FCM-PCA

The GRNN (see Fig. 6) is one type of radial basis function (RBF) networks based on the kernel regression [2] and is a robust regression tool for its strong nonlinear mapping capability and high training speed. Also, it overcomes the shortcoming of back propagation neural network which needs a large number of training samples. It is suitable for a problem with limited training samples, and GRNN has been proved to be a useful tool to perform prediction and comparison in many fields [6, 14, 18]. Briefly, the structure of GRNN is composed of four layers: an input layer, a pattern layer, summation layer, and output layer. The first input layer consists of reduced input variables from FCM-PCA preprocess that connected to the second pattern layer. The neurons in the pattern layer can memorize the relationship between the neuron of entry and the proper response of pattern layer. The two summations $\mathbf{S_s}$ and $\mathbf{S_w}$ in the summation layer compute the arithmetic sum of the pattern outputs with the interconnection weight equals to one and compute the weighted sum of the pattern layer outputs with the interconnection weight, respectively. The neurons in the summation layer are then summed and fed into the output layer. The number of the neurons in the output layer equals to the dimension of the output vector. Since there are five clusters in each frequency, there are a total number of thirty-five GRNN predictors for the seven frequencies.

The primary function of GRNN [2] is to estimate a linear or nonlinear regression surface on independent variables. It assumes the continuous probability density function $f(\mathbf{X}^j, y^j)$ has a random variable $\tilde{\mathbf{X}}^j$ and $\tilde{y}^j$. The corresponding regression of y^j on $\mathbf{X}^j$ [2] is given by:

$$E\left[y^j/\mathbf{X}^j\right] = \frac{\int_{-\infty}^{\infty} y^j f(\mathbf{X}^j, y^j) dy}{\int_{-\infty}^{\infty} f(\mathbf{X}^j, y^j) dy} \tag{13}$$

where $\mathbf{X}^j$ refers to the data matrix $\mathbf{X}$ in jth cluster.

The probability density function $f(\mathbf{X}^j, y^j)$ is estimated by Parzen nonparametric estimator from $\mathbf{X}^j$ and y^j using the reduced $\bar{N}^j$ observation samples (that is less than the original number of samples, N^j in each cluster). l^j (less than the original number of input variables, n in each cluster). The probability estimator $\hat{f}(\mathbf{X}^j, y^j)$ is based on the sample values $\mathbf{X}^j$ and y^j of the random variable $\tilde{\mathbf{X}}^j$ and $\tilde{y}^j$, respectively. The probability density function $\hat{f}(\mathbf{X}^j, y^j)$ [2] is expressed as:

$$\hat{f}(\mathbf{X}^j, y^i) = \frac{1}{(2\pi)^{\frac{l^j+1}{2}} \sigma^{l^j+1}} \cdot \frac{1}{\bar{N}^j} \sum_{i=1}^{\bar{N}^j} \exp\left[-\frac{\left\|\left(\mathbf{X}^j - \tilde{\mathbf{X}}^j\right)\right\|}{2\sigma^2}\right] \cdot \exp\left[-\frac{\left\|(y^j - \tilde{y}^j)\right\|^2}{2\sigma^2}\right] \tag{14}$$

A spread parameter σ is assigned to $\mathbf{X}^j$ and y^j of j^{th} cluster. The resulting regression [2] in (15) involves summations over the observations.

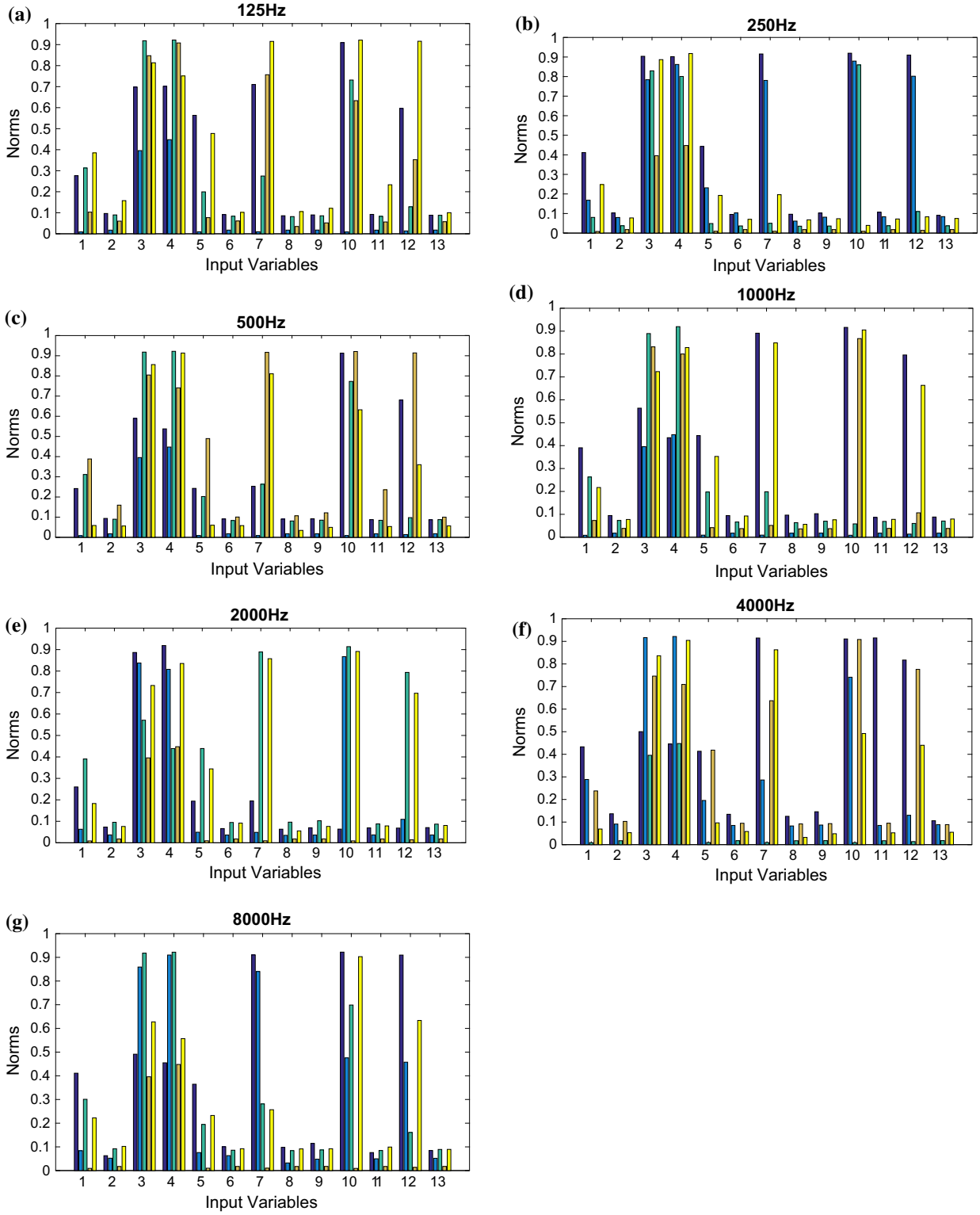

Fig. 5 Leverage scores of each input parameter for each cluster group at different frequencies (cluster 1: *dark blue*, cluster 2: *blue*, cluster 3: *cyan*, cluster 4: *Orange*, and cluster 5: *yellow*). **a** 2-norm distribution for input parameter across each cluster group at 125 Hz, **b** 2-norm distribution for input parameter across each cluster group at 250 Hz, **c** 2-norm distribution for input parameter across each cluster group at 500 Hz, **d** 2-norm distribution for input parameter across each cluster group at 1000 Hz, **e** 2-norm distribution for input parameter across each cluster group at 2000 Hz, **f** 2-norm distribution for input parameter across each cluster group at 4000 Hz, and **g** 2-norm distribution for input parameter across each cluster group at 8000 Hz (color figure online)

Table 3 Selection of input variables in clusters

Freq. (Hz)	Clusters	Total sound power level (dBA)	Room type	Room surface area (m^2)	Room volume, V (111^3)	Nearest source 1 SWL, dBA	Dist to nearest source 1	Nearest source 2 SWL, dBA
125	1	O	X	O	O	O	X	O
	2	X	O	O	O	X	O	X
	3	O	X	O	O	O	X	O
	4	O	X	O	O	O	X	O
	5	O	O	O	O	O	X	O
250	1	O	X	O	O	O	X	O
	2	O	X	O	O	O	X	O
	3	O	X	O	O	X	X	X
	4	X	O	O	O	X	O	X
	5	O	O	O	O	O	O	O
500	1	O	O	O	O	O	X	O
	2	X	O	O	O	X	O	X
	3	O	X	O	O	O	X	O
	4	O	O	O	O	O	X	O
	5	X	X	O	O	X	X	O
1000	1	O	X	O	O	O	X	O
	2	X	O	O	O	X	O	X
	3	O	O	O	O	O	X	O
	4	O	X	O	O	X	X	O
	5	O	X	O	O	O	X	O
2000	1	O	O	O	O	O	X	O
	2	O	X	O	O	O	X	O
	3	O	X	O	O	O	X	O
	4	X	O	O	O	X	O	X
	5	O	X	O	O	O	X	O
4000	1	O	X	O	O	O	X	O
	2	O	X	O	O	O	X	O
	3	X	O	O	O	X	O	X
	4	O	X	O	O	O	X	O
	5	X	X	O	O	O	X	O
8000	1	O	X	O	O	O	X	O
	2	O	X	O	O	O	O	O
	3	O	X	O	O	O	X	O
	4	X	O	O	O	X	O	X
	5	O	O	O	O	O	X	O

Freq.(Hz)	Dist. To nearest source 2	Mean absorption coefficient	Max sound power level of adjacent room (dBA)	Room type of adjacent room	Panel/insulation thickness between adjacent room (mm)	Number of decks to main deck	No. of dominant input variables	No. of samples (total 424 samples for each freq)
125	X	X	O	X	O	X	7	48
	O	O	X	O	X	O	8	205
	X	X	O	X	O	X	7	61
	X	X	O	X	O	X	7	66
	X	X	O	O	O	X	9	44

Table 3 continued

Freq.(Hz)	Dist. To nearest source 2	Mean absorption coefficient	Max sound power level of adjacent room (dBA)	Room type of adjacent room	Panel/insulation thickness between adjacent room (mm)	Number of decks to main deck	No. of dominant input variables	No. of samples (total 424 samples for each freq)
250	X	X	O	X	O	X	7	25
	X	X	O	X	O	X	7	54
	X	X	O	X	O	X	5	83
	O	O	X	O	X	O	8	57
	X	O	X	O	O	O	8	205
500	X	X	O	X	O	X	8	66
	O	O	X	O	X	O	8	205
	X	X	O	X	O	X	7	44
	X	X	O	O	O	X	9	48
	X	X	O	X	O	X	5	61
1000	X	X	O	X	O	X	7	48
	O	O	X	O	X	O	8	66
	X	O	X	X	X	O	8	205
	X	X	O	X	O	X	6	61
	X	X	O	X	O	X	7	44
2000	X	O	X	O	X	O	9	76
	X	X	O	X	O	X	7	61
	X	X	O	X	O	X	7	205
	O	O	X	O	X	O	8	48
	X	X	O	X	O	X	7	34
4000	X	O	O	O	O	X	9	66
	X	X	O	X	O	X	7	44
	O	O	X	O	X	O	8	205
	X	X	O	X	O	X	7	61
	X	X	O	X	O	X	6	48
8000	X	X	O	X	O	X	7	70
	X	X	O	X	O	X	8	38
	X	X	O	X	O	X	7	205
	O	O	X	O	X	O	8	76
	X	X	O	O	O	X	9	35

"x" refers to variable removed while "o" refers to the dominant variables to retain for subsequent GRNN training

$$\hat{\mathrm{Y}}^{j}(\mathbf{X}^{j}) = \frac{\sum_{i=1}^{\bar{N}^{j}} \tilde{y}^{j} \exp\left(-\frac{D_i^{j2}}{2\sigma^2}\right)}{\sum_{i=1}^{\bar{N}^{j}} \exp\left(-\frac{D_i^{j2}}{2\sigma^2}\right)} \tag{15}$$

where the two norms of scalar function $D_i^{j2} = \left\| \left(\mathbf{X}^{j} - \tilde{\mathbf{X}}^{j} \right) \right\|$.

The "spread" refers to the spread of radial basis functions which plays a significant role in FCM-PCA-GRNNs function approximation [2]. The larger spread gives a smoother function approximation while the smaller spread fits the data closely. The optimal spread variables can be selected based on prior knowledge or intelligent optimization algorithms [5]. In this study, a *k*-fold cross-validation method is used to find the corresponding spread parameter for each neuron based on the training samples in the clusters. The selected value of spread parameter is chosen once the error of the validation data starts to increase. It is the point where overtraining of the network may occur. The mean squared error (MSE) criteria measure the difference between the estimated and target. An updated spread parameter $\sigma_{i+1} = \sigma_i + i \times \theta$ with θ is the adjustable learning factor and i is the current loop index.

In each cluster, the data samples are randomly divided into training and validation set with the following weighting of 80 and 20%, respectively, for each cluster (see Fig. 1). The validation set is used as an additional independent measurement to estimate the quality of the

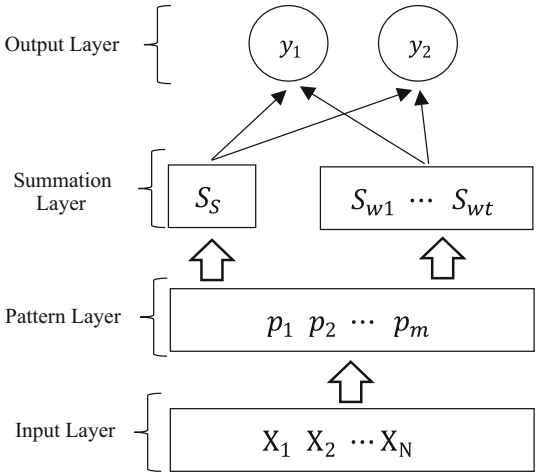

Fig. 6 Architectural implementation of multiple GRNN after FCM-PCA

trained network. In the *k*-fold cross-validation, the original sample is randomly partitioned into similar-sized subsamples. In the subsamples, one subsample is used as the validation data for testing the model, and the remaining subsamples as training data. After a maximum of four iterations (from 0.01 to 3 with a step size of 0.01) for each cluster at 125, 250, 500, 1000, 2000, 4000, and 8000 Hz, the optimal spread variables that give the minimum MSE are chosen. For the sake of clarity, Fig. 7 illustrates the MSE of five clusters across different spread variables ranging 0.01–3 for 125 and 250 Hz. The optimal spread variables for each group are different. Typically, the FCM-PCA-GRNNs tend to perform better with a smaller the spread parameter than a larger value. As a result, the optimal spread parameter is approximately 0.001 for all frequencies.

7 Results and discussion

The data samples are randomly divided into training and validation set with the following weighting of 80 and 20%, respectively, for each cluster (see the earlier proposed architecture in Fig. 1). The optimal spread parameters are determined in Sect. 6, and the predicted SPLs are compared with the SEA-DF simulation from the validation set. The comparisons of spatial SPL and spatial average SPL are compared in the following octave frequency bands: 125, 250, 500, 1000, 2000, 4000, and 8000 Hz as shown in Fig. 8. The predicted, simulated spatial SPL and spatial average SPL are compared. The maximum and minimum noise levels, data distribution, and the data mean are quite consistent. The results imply the proposed FCM-PCA-GRNNs is able to predict the SPL quite accurately as compared with the SEA-DF simulation.

As seen in Table 4, the maximum and the mean value of the errors at each frequency are tabulated to analyze the prediction performance of the proposed method. Table 4 presents the worst possible prediction results for spatial and spatial average occur at 1000 Hz. The errors of 1.8 and 1.75 dB can be determined in the maximum spatial and spatial average, respectively. The mean errors of the spatial and spatial average are 0.04 dB (8000 Hz) and 0.025 dB (4000 Hz), respectively. The error is well below the accepted limit of 3 dB for engineering survey method. As seen in the prediction error tabulated in Table 5, the error of FCM-PCA-GRNNs is quite small as compared to GRNNs for the spatial average at each frequency. The proposed FCM-PCA-GRNNs approach can predict the spatial and the spatial average noise level. Note that the training and validation sets are selected

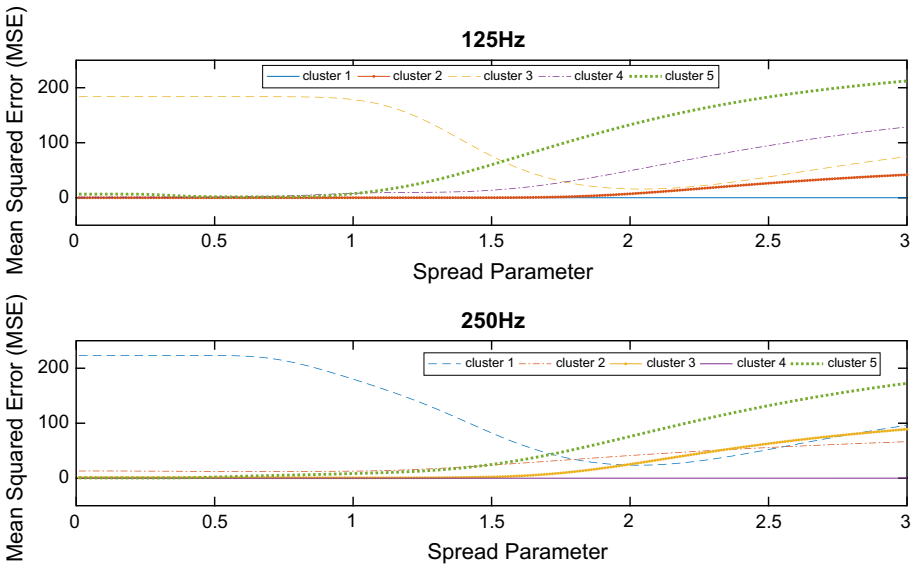

Fig. 7 MSE of five clusters in 125 and 250 Hz after FCM-PCA-GRNNs

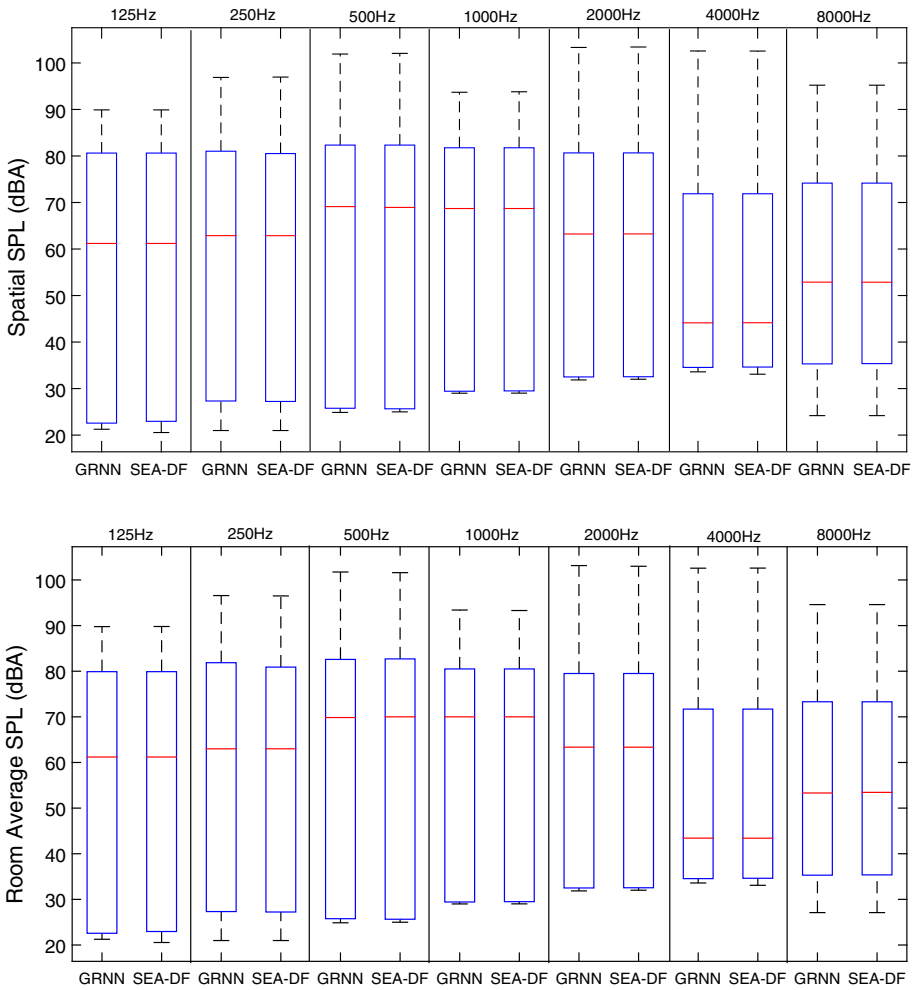

Fig. 8 Comparisons of **a** spatial SPL and **b** spatial average SPL between FCM-PCA-GRNNs prediction and SEA-DF simulation

Table 4 Summary of prediction errors between FCM-PCA-GRNNs and SEA-DF

Center frequency (Hz)	Error (dB)			
	Max spatial	Mean spatial	Max spatial average	Mean spatial average
125	0.9	−0.016	0.9	0.02
250	0.7	0.01	0.7	−0.02
500	1.4	−0.01	1.3	−0.02
1000	1.8	0.03	1.75	0.01
2000	1.1	−0.02	1.05	0.02
4000	0.6	0.007	0.55	0.025
8000	0.7	0.04	0.66	0

randomly such that the cross-validation can select the optimal spread value for each run. It ensures the proposed FCM- the PCA-GRNNs model is an optimal and robust for the data set.

The use of FCM-PCA on samples has significantly improved the multiple GRNN models performance, i.e., FCM-PCA-GRNNs. Table 5 presents the average absolute prediction error for the spatial SPL and spatial average SPL before and after using FCM-PCA. It shows the improvement in the spatial error of 0.14–0.42 dB, while the improvement in the spatial average error is 0.21–0.43 dB. Additionally, the error fluctuation in different frequencies has been reduced. By defining the percentage of improvement, Fig. 9 shows an average percent improvement of minimal 25 and 85% in spatial and spatial average SPL, respectively, across all the frequencies. With the optimal GRNNs obtained, the use of FCM-PCA to pre-processing the input parameters enhances the reliability

Table 5 Model performance with and without FCM-PCA preprocessing

Frequency (Hz)	Description	SPL (dB)		Error in SPL (dB)		% of improvement using FCM-PCA-GRNNs	
		Spatial	Spatial average	Spatial	Spatial average	Spatial	Spatial average
125	GRNN	0.62	0.50	0.38	0.43	61	86
	FCM-PCA-GRNNs	0.24	0.07				
250	GRNN	0.54	0.29	0.19	0.25	35	86
	FCM-PCA-GRNNs	0.35	0.04				
500	GRNN	0.73	0.33	0.37	0.30	50	90
	FCM-PCA-GRNNs	0.36	0.03				
1000	GRNN	0.56	0.33	0.21	0.32	37	96
	FCM-PCA-GRNNs	0.35	0.01				
2000	GRNN	0.54	0.25	0.14	0.21	25	86
	FCM-PCA-GRNNs	0.40	0.04				
4000	GRNN	0.68	0.44	0.42	0.43	62	98
	FCM-PCA-GRNNs	0.26	0.01				
8000	GRNN	0.46	0.27	0.19	0.26	40	96
	FCM-PCA-GRNNs	0.27	0.01				

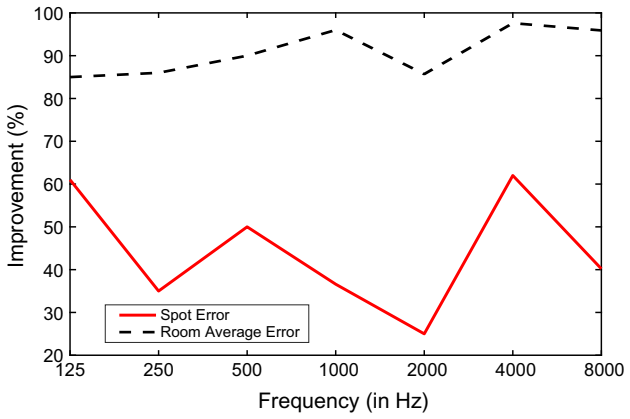

Fig. 9 Performance improvement for FCM-PCA-GRNNs as compared to GRNNs only

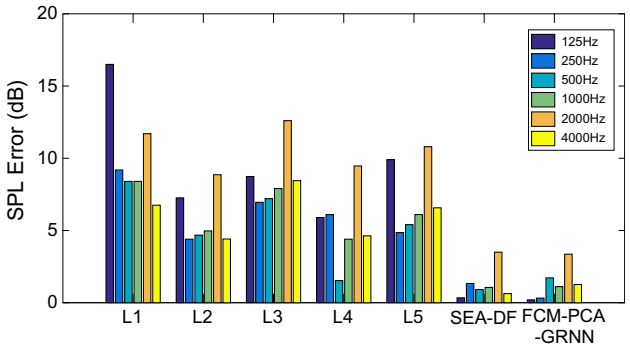

Fig. 10 Prediction error between FCM-PCA-GRNNs, SEA-DF, and empirical acoustic models for engine room

and robustness of the prediction model as more relevant parameters and multiple GRNN models are used.

The proposed FCM-PCA-GRNNs model performance is further evaluated by the actual measurement using the real engine room case study [9]. The structural and acoustic information of the engine room associated with the thirteen input variables is collected as the test samples. The frequency-dependent spatial SPL and spatial average SPL are directed mapped. As shown in Fig. 10, the result from FCM-PCA-GRNNs model is compared with the empirical acoustic models such as Thompson model (L1), Kuttruff model (L2), SNAME method (L3), Heerema and Hodgson model (L4), Sergeyev model (L5), and SEA-DF. It shows that FCM-PCA-GRNNs noise model exhibits at least 16% less error than the SEA-DF and empirical-based acoustic models. In summary, FCM-PCA-GRNNs provides a comparable and more robust model for noise prediction at much lower cost as compared to commercial CAD modeling using SEA-based software.

8 Conclusion

This paper proposed a modified multiple GRNN model with FCM and principal component analysis (PCA) before training to improve the performance of the GRNN models. The sound pressure level (SPL) on various compartments onboard of a jack-up rig is influenced by many uncertain acoustical parameters. The

implementation of the FCM-PCA groups the data samples into clusters with less and more relevant input variables by removing the less correlated parameters from the clusters in each frequency. With the FCM-PCA preprocessing, the FCM-PCA-GRNNs prediction accuracy has improved the spatial and spatial average SPL by approximately 0.14–0.42 dB and 0.21–0.43 dB, respectively. The spread parameters are identified by cross-validation with minimum root mean squared error to ensure the FCM-PCA-GRNNs are an optimal and reliable predictor for the multiple frequency-dependent data. In the engine room study, the FCM-PCA on the fused multiple GRNN models exhibits less than 16% in the SPL error as compared to commercial acoustic software using statistical energy analysis (SEA) and empirical-based acoustics models. The FCM-PCA-GRNNs are useful when the room arrangement tends to change too frequently due to different design requirements from owner and designers during the preliminary design stage. Hence, the proposed FCM-PCA-GRNNs model helps to predict the SPL of different compartments effectively at different frequencies as it consumes less time and resources when compared to the commercial acoustics software that requires approximately 2–3 months to build the functional acoustics model.

For future works, the proposed model will be further optimized and improved. More works will be done to improve the FCM partition and fuzzy membership functions for the multiple frequency-dependent data set.

Acknowledgements The authors would like to thank the Singapore Maritime Institute (ID: SMI-2015-MA-11) for sponsoring and supporting the project.

Compliance with ethical standards

Conflict of interest The authors declare that there is no conflict of interest.

References

1. Nilsson AC (1978) Noise prediction and prevention in ships, New York
2. Specht DF (1991) A general regression neural network. IEEE Trans Neural Netw 2(6):568–576
3. Hamoda MF (2008) Modeling of construction noise for environmental impact assessment. J Constr Dev Ctries 13(1):79–89
4. Nirmal J, Zaveri M, Patnaik S, Kachare P (2014) Voice conversion using general regression neural network. Appl Soft Comput 24:1–12
5. Liu JL, Bao W, Shi L, Zuo BQ, Gao WD (2014) General regression neural network for prediction of sound absorption coefficients of sandwich structure nonwoven absorbers. Appl Acoust 76:128–137
6. Djarfour N, Ferahtia J, Babaia K, Baddari E, Said A, Farfour M (2014) Seismic noise filtering based on generalized regression neural networks. Comput Geosci 69:1–9
7. Chatillon J (2008) Influence of source directivity on noise level in industrial halls: simulation and experiments. Appl Acoust 68(6):682–698
8. Hodgson M (2003) Ray-tracing evaluation of empirical models for predicting noise in industrial workshops. Appl Acoust 64(11):1003–1048
9. Ji X, Chin CS (2015) Analysis of acoustic models and statistical energy analysis with direct field for machinery room on offshore platform. Acta Acust united Acust 1244(101):1234–1244
10. Azma P, Munawir A, Mohamad W, Mohammad J (2013) The effect of direct field component on a statistical energy analysis (SEA) model. Appl Mech Mater 471:279–284
11. Heerema N, Hodgson M (1999) Empirical models for predicting noise levels, reverberation times and fitting densities in industrial workshops. Appl Acoust 57(1):51–60
12. Mirenberg KJ (2011) Architectural Acoustic modeling of ship noise and sound field mapping. Sound Vib 5:6–10
13. Wu ZD, Xie WX, Yu JP (2003) Fuzzy C-mean cluster algorithm based on kernel method. In: Proceedings of the fifth international conference on computational intelligence and multimedia applications. Xi'an, China
14. Strehl A (2002) Relationship-based clustering and cluster ensembles for high-dimensional data mining. The University of Texas at Austin, PhD Dissertation
15. Ghosh S, Dubey SK (2013) Comparative analysis of K-means and fuzzy C-means algorithms. Int J Adv Comput Sci Appl 4(4):35–39
16. Heinrich J, Weiskopf D (2013) State of the art of parallel coordinates. In: Eurographics 2013. Girona, Spain
17. Lu YH, Ma TH, Yin CH, Xie XY, Tian W, Zhong SM (2013) Implementation of the fuzzy C-means clustering algorithm in meteorological data. Int J Database Theory Appl 6(5):1–18
18. Ozturk AU, Turan ME (2012) Prediction of effects of microstructural phases using generalized regression neural network. Constr Build Mater 29:279–283